SCIENTIFIC CULTURE
www.sci-cult.com

SCIENTIFIC CULTURE, Vol. 12, No. 4, (2026), pp. 2549-2556
Open Access. Online & Print

DOI: 10.5281/zenodo.12426330

HYDROCLIMATIC ANALYSIS OF THE VINCES RIVER BASIN USING OFFICE AND GEOMATIC TOOLS

Carmen Alexandra Sinchi-Rivas[1]*, Alfredo José Cañas-Suárez[2], Carlos Alberto Nieto-Cañarte[3], Pedro Harrys Lozano-Mendoza[3], Roberto Johan Barragán-Monrroy[3], Víctor Manuel Guamán-Sarango[3], Mayra Lisette Zapata-Velasco[4]

[1]Universidad Estatal de la Península de Santa Elena
[2]Universidad de Guayaquil
[3]Universidad Técnica Estatal de Quevedo
[4]Universidad Estatal del Sur de Manabí

Received: **10/10/2025**
Accepted: **08/03/2026**

Corresponding Author: Carmen Alexandra Sinchi-Rivas (csinchi5208@upse.edu.ec)

ABSTRACT

The hydroclimatic analysis of the Vinces River basin focused on assessing hydrological and climatic characteristics through the use of office and geomatic tools, such as HYDROGNOMON and Geographic Information Systems (GIS). The basin, located in west-central Ecuador, covers an area of approximately 4600 km² and comprises 12 cantons distributed in four provinces. The hydrological and meteorological data, provided by the National Institute of Meteorology and Hydrology of Ecuador (INAMHI), were processed to determine the theoretical probability distribution that best fits the annual rainfall in key seasons. The results revealed that the Normal distribution is better suited to the M0006 station, while the Log-Pearson III distribution is more suitable for the M0124 station. These distributions allowed the calculation of the Intensity-Duration-Frequency (IDF) curves, necessary for the hydrological design in the region. In addition, the analysis identified the spatial variations of temperature, precipitation, solar radiation and wind speed within the basin. The research highlights the importance of employing comprehensive methodologies and the need for calibration and validation of hydrological models to minimize uncertainty in water resource management. The study concludes that the Vinces River basin, as part of the Guayas River network, is vulnerable to hydroclimatic fluctuations that can impact water supply and integrated water management, requiring adaptation measures to ensure the sustainability of the resource.

KEYWORDS: Hydroclimatology, Vinces River Basin, Hydrological Models, Probability Distribution, Water Resource Management.

1 INTRODUCTION

Watersheds are defined as physically and/or politically delimited natural areas where various human activities occur (Allali et al., 2022). These areas serve as a territorial unit for planning or ordering due to the continuous interaction between nature and human activity (Hamel et al., 2017). In this sense, the pursuit of sustainability is paramount to ensure the preservation of this territorial unit's harmony (Garcia et al., 2024). Theoretically, sustainable development is defined as the equitable balance of social, economic, and environmental factors (Gunay et al., 2024).

The preservation and maintenance of natural environments, particularly the coordinated administration of water resources, constitutes a global challenge. This challenge arises from the environment's inherent limitations and its significance from social, economic, and environmental standpoints (Hao et al., 2023). In general, solutions are being sought worldwide to achieve sustainable development, with efforts focused on monitoring social, economic, and environmental factors, given their interdependence (Lutz et al., 2016). The expanding human population on Earth is proportional to the demand for freshwater, as its use is indispensable and occurs daily (in domestic, agricultural, and industrial contexts). Due to the complex dynamics of this resource, it is crucial to implement an integrated management strategy that can adapt to changes in space and time (Nasiri-Khiavi et al., 2024).

It is imperative to acknowledge the interconnection between economic advancement and water consumption, particularly given the escalating demands for water resulting from human activities, which can precipitate conflicts over its utilization (Arsenault et al., 2023). However, it is imperative to consider other valuations of the water resource that extend beyond its economic value, given its multifaceted applications (Greenwood & Eimers 2023). Consequently, integrated water resource management (IWRM) must encompass multi-objective analysis that incorporates aspects of "social, economic, and environmental" sustainability (Prinsloo et al., 2023).

Shahed-Behrouz et al. (2023) emphasize that selecting an appropriate probabilistic model that can effectively predict the behavior of a hydroclimatic variable requires access to precipitation, evapotranspiration, temperature, and flow data, in addition to a comprehensive understanding of the underlying physical principles. In these models, it is necessary to obtain the measurements and perform a goodness-of-fit test (Jiang et al., 2024), which will indicate how adequate the chosen probabilistic model is. The model can be used to forecast with some occasional possibility of a hydrometeorological phenomenon with a certain magnitude or to determine its magnitude for a specific phase of occurrence (Staniszewska et al., 2022). Some of the hypothetical distributions frequently employed in hydrography include: normal; log-normal of 2 or 3 parameters; gamma of 2 or 3 parameters; log-Pearson type III; Gumbel and log-Gumbel (Tran et al., 2024).

In recent years, there has been an increasing utilization of computer tools and hydrographic modelers that have been integrated with Geographic Information Systems (GIS). These tools facilitate the evaluation of soil and water within a natural territory (basin) and their anthropogenic interaction, enabling the comprehension and management of a river system. The outcomes of these analyses are employed in temporal, medium, and extended-term projections, ensuring the availability of vital resources for both present and future generations downstream of the basin (Zhang et al., 2011).

2 MATERIALS AND METHODS

The research was carried out in the Vinces River basin, with an area of around 4,600 km², located in the center-west of Ecuador. The projected coordinates UTM X/Y (East/North) are: 630000m / 9980000m and 740000m / 9780000m; or in geographical coordinates: 79º49'54.475"W / 0º10'51.27"S and 78º50'32.645"W / 1º59'20.334"S (Figure 1). Twelve cantons are under the influence of the basin: Santo Domingo; Pujilí, Sigchos, La Maná; Buena Fe, Valencia, Quevedo, Mocache, Palenque, Vinces, Baba; Saltpetre. These cantons are distributed among the provinces of Santo Domingo de los Tsáchilas, Cotopaxi, Los Ríos (concentrating most of the territory of the basin) and Guayas.

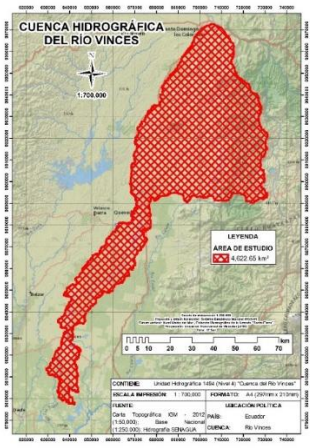

Figure 1. Study area (Vinces River basin)

The hydrological and meteorological information used in the research was extracted and tabulated from the YEARBOOKS of the National Institute of Meteorology and Hydrology of Ecuador "INAMHI" (Table 1). The modeling will be carried out with the HYDROGNOMON program, which will allow understanding how climatic variations can affect water supply, water resource management and the forecast of hydrological risks for the influx site in the hydrobasin; procedures presented by Mahmood et al. (2024).

Table 1. Erosion levels esablished by FAO

Code	Season	Guy	Latitude	Longitude	Elevation
H0347	Quevedo	Hydrological	-1.015	-79.463	100 meters above sea level
H0348	Vinces	Hydrological	-1.549	-79.751	41 meters above sea level
M0006	Pichilingue	Weather	-1.090	-79.468	120 meters above sea level
M0124	San Juan	Weather	-0.954	-79.319	95 meters above sea level
Source: INAMHI (2024)					

The study area (Vinces River basin) has a temperature range of 5.30-25.60ºC (Figure 2), precipitation of 768-2831mm (Figure 3), solar radiation of 11642-16013kJ/m²/day (Figure 4), and wind speed of 1.30-4.02m/s (Figure 5). Below are the different elements of the weather.

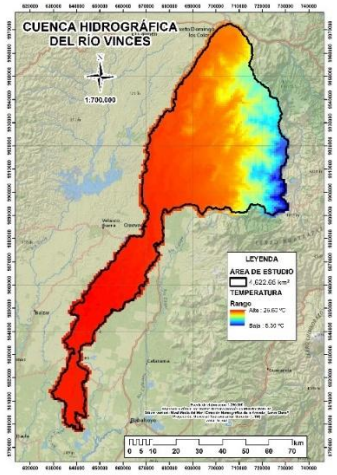

Figure 2. Average temperatura

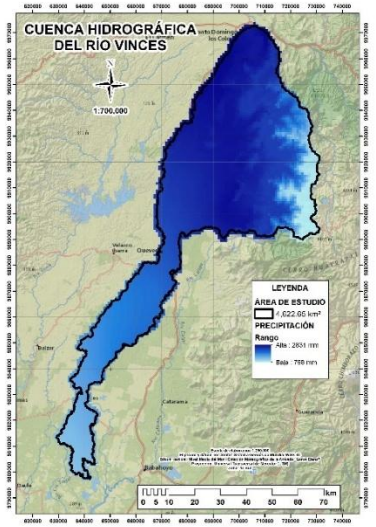

Figure 3. Average rainfall

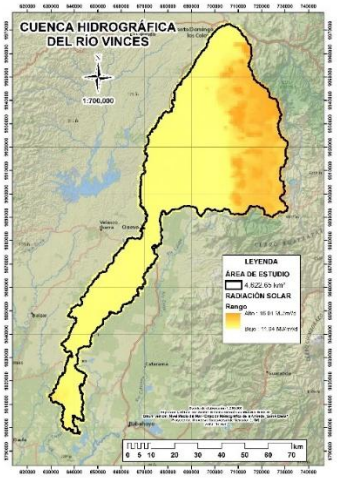

Figure 4. Average solar radiation

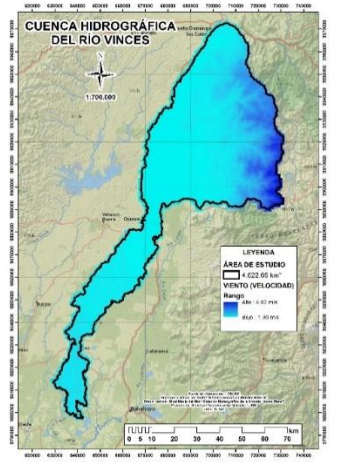

Figure 5. Wind Speed

The basin of the Vinces River is made up of several tributaries (tributaries), which take different names along its course, from the north it begins as the Baba River, Lulo River and San Pablo River, which form the Quevedo River, where downstream it takes the name of Mocache River and at the mouth of the basin, the river takes its name from the canton that crosses "Vinces" (Figure 6). It is important to note that this

basin is one of the seven that form the exorheic basin (whose waters go to the sea) of the Guayas River. The Guayas River is the most important river system on the southwestern Pacific coast and its drainage network originates in the western derivations of the Andes Mountains and on the eastern slopes of the Chongón-Colonche Coastal Mountain Range. The Daule and Babahoyo rivers are part of this network and join five kilometers from the city of Guayaquil to form the Guayas River (Figure 7). Figures 6 and 7 show hydrographic maps.

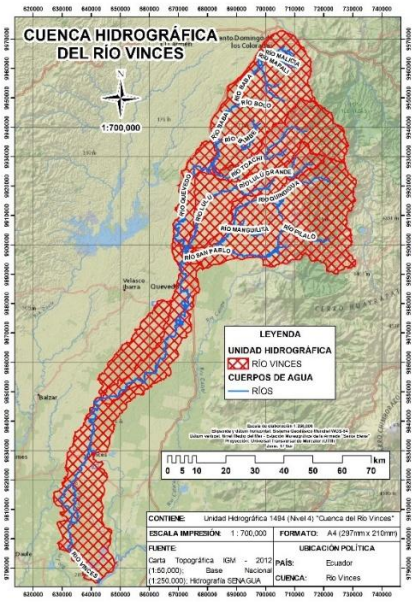

Figure 6. Rivers of the basin

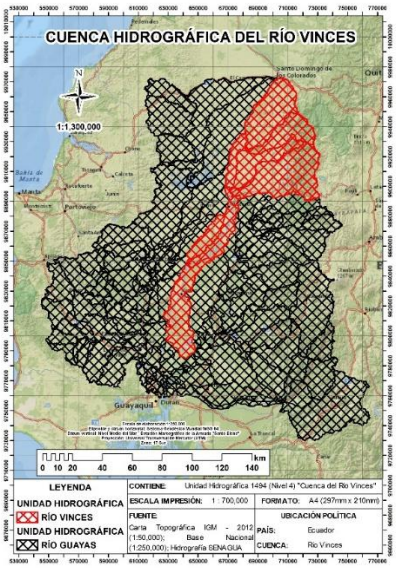

Figure 7. Guayas River Basin

3 RESULT AND DISCUSSION

According to the results obtained from the office analysis in HYDROGNOMON, in order to know the THEORETICAL DISTRIBUTION OF PROBABILITY that best fits the annual data of maximum precipitation in 24 hours of the M0006 station (Table 2 and 3) and based on the Chi-square (60.65%) and Kolmogorov-Smirnov (97.50%) statistical test, it is a NORMAL distribution. It is worth mentioning that N = 24, Rank = 98.70 and Class Number = 5.23 ≅ 5. This allows us to obtain the IDF Curve for different maximum return periods (Tables 4 and 5; Figure 8):

Table 2. Probable maximum daily rainfall for M0006

Return Period	Precipitation	Probability of occurrence	Fixed interval correction
T	**P**	**F (P)**	**1.13 P**
2 years	128.80 mm	50.00%	145.55 mm
5 years	153.59 mm	80.00%	173.55 mm
10 years	166.54 mm	90.00%	188.19 mm
25 years	180.35 mm	96.00%	203.80 mm
50 years	189.28 mm	98.00%	213.88 mm
100 years	197.30 mm	99.00%	222.95 mm
500 years	213.55 mm	99.80%	241.31 mm

Table 3. Maximum rainfall for M0006

Duration Time "D"	Coefficient	Years						
		2	**5**	**10**	**25**	**50**	**100**	**500**
24 hours	100%	145.55	173.55	188.19	203.80	213.88	222.95	241.31
18 hours	91%	132.45	157.93	171.25	185.46	194.63	202.89	219.60
12 hours	80%	116.44	138.84	150.55	163.04	171.11	178.36	193.05
8 hours	68%	98.97	118.02	127.97	138.58	145.44	151.61	164.09
6 hours	61%	88.78	105.87	114.80	124.32	130.47	136.00	147.20
5 hours	57%	82.96	98.92	107.27	116.17	121.91	127.08	137.55
4 hours	52%	75.69	90.25	97.86	105.98	111.22	115.94	125.48
3 hours	46%	66.95	79.83	86.57	93.75	98.39	102.56	111.00
2 hours	39%	56.76	67.69	73.39	79.48	83.41	86.95	94.11
1 hour	30%	43.66	52.07	56.46	61.14	64.16	66.89	72.39

Table 4. Rainfall intensity for M0006

Duration Time	Rainfall intensity as a function of the Return Period "I" (mm/h)						
	2 years	5 years	10 years	25 years	50 years	100 years	500 years
24 hours	6.06	7.23	7.84	8.49	8.91	9.29	10.05
18 hours	7.36	8.77	9.51	10.30	10.81	11.27	12.20
12 hours	9.70	11.57	12.55	13.59	14.26	14.86	16.09
8 hours	12.37	14.75	16.00	17.32	18.18	18.95	20.51
6 hours	14.80	17.64	19.13	20.72	21.74	22.67	24.53
5 hours	16.59	19.78	21.45	23.23	24.38	25.42	27.51
4 hours	18.92	22.56	24.46	26.49	27.80	28.98	31.37
3 hours	22.32	26.61	28.86	31.25	32.80	34.19	37.00
2 hours	28.38	33.84	36.70	39.74	41.71	43.48	47.06
1 hour	43.66	52.07	56.46	61.14	64.16	66.89	72.39

Table 5. IDF (Intensity - Duration - Frequency) curve for M0006

T	Duration of precipitation "t" (mm/h)											
	5 min	10 min	15 min	20 min	25 min	30 min	35 min	40 min	45 min	50 min	55 min	60 min
2 years	220.51	143.84	112.03	93.83	81.77	73.08	66.45	61.20	56.92	53.34	50.29	47.67
5 years	238.84	155.80	121.35	101.63	88.57	79.15	71.98	66.29	61.65	57.77	54.48	51.63
10 years	253.72	165.50	128.90	107.96	94.08	84.08	76.46	70.42	65.49	61.37	57.87	54.85
25 years	274.82	179.27	139.62	116.94	101.91	91.08	82.82	76.28	70.94	66.48	62.68	59.41
50 years	291.94	190.43	148.32	124.22	108.26	96.75	87.98	81.03	75.35	70.62	66.59	63.11
100 years	310.12	202.29	157.56	131.96	115.00	102.78	93.46	86.08	80.05	75.01	70.73	67.04
500 years	356.83	232.76	181.29	151.83	132.32	118.26	107.54	99.04	92.10	86.31	81.39	77.14

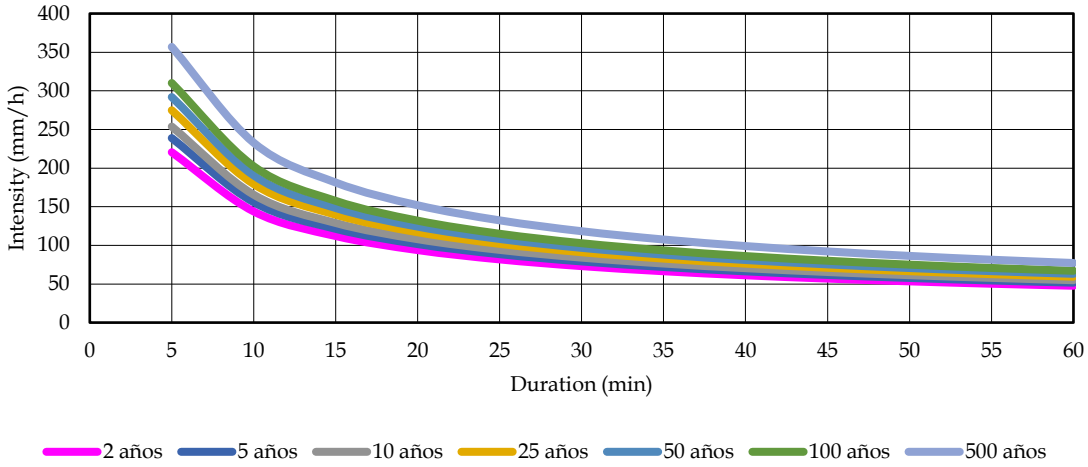

Figure 8. IDF (Intensity - Duration - Frequency) curve for M0006

According to the results obtained from the office analysis in HYDROGNOMON, to know the THEORETICAL DISTRIBUTION OF PROBABILITY that best fits the annual data of maximum precipitation in 24 hours of the M0124 station (Tables 6 and 7) and based on the Chi-square (44.50%) and Kolmogorov-Smirnov (99.97%) statistical test, it is a LOG PEARSON III distribution. It is worth mentioning that N = 24, Rank = 142.20 and Class Number = 5.23 ≅ 5. This allows us to obtain the IDF Curve for different maximum return periods (Tables 8 and 9; Figure 9):

Table 6. Probable maximum daily rainfall for M0124

Return Period	Precipitation	Probability of occurrence	Fixed Interval Correction
T	P	F (P)	1.13 P
2 years	114.84 mm	50.00%	129.77 mm
5 years	149.07 mm	80.00%	168.45 mm
10 years	172.63 mm	90.00%	195.07 mm
25 years	203.49 mm	96.00%	229.94 mm
50 years	227.31 mm	98.00%	256.86 mm
100 years	251.88 mm	99.00%	284.62 mm
500 years	312.81 mm	99.80%	353.47 mm

Table 7. Maximum rainfall for M0124

Duration Time "D"	Coefficient	Years						
		2	5	10	25	50	100	500
24 hours	100%	129.77	168.45	195.07	229.94	256.86	284.62	353.47
18 hours	91%	118.09	153.29	177.51	209.25	233.75	259.01	321.66
12 hours	80%	103.82	134.76	156.05	183.95	205.49	227.70	282.78
8 hours	68%	88.25	114.55	132.65	156.36	174.67	193.54	240.36
6 hours	61%	79.16	102.75	118.99	140.26	156.69	173.62	215.62
5 hours	57%	73.97	96.02	111.19	131.07	146.41	162.23	201.48
4 hours	52%	67.48	87.59	101.44	119.57	133.57	148.00	183.80
3 hours	46%	59.70	77.49	89.73	105.77	118.16	130.93	162.60
2 hours	39%	50.61	65.70	76.08	89.68	100.18	111.00	137.85
1 hour	30%	38.93	50.54	58.52	68.98	77.06	85.39	106.04

Table 8. Rainfall intensity for M0124

Duration Time	Rainfall intensity as a function of the Return Period "I" (mm/h)						
	2 years	5 years	10 years	25 years	50 years	100 years	500 years
24 hours	5.41	7.02	8.13	9.58	10.70	11.86	14.73
18 hours	6.56	8.52	9.86	11.62	12.99	14.39	17.87
12 hours	8.65	11.23	13.00	15.33	17.12	18.97	23.56
8 hours	11.03	14.32	16.58	19.55	21.83	24.19	30.04
6 hours	13.19	17.13	19.83	23.38	26.11	28.94	35.94
5 hours	14.79	19.20	22.24	26.21	29.28	32.45	40.30
4 hours	16.87	21.90	25.36	29.89	33.39	37.00	45.95
3 hours	19.90	25.83	29.91	35.26	39.39	43.64	54.20
2 hours	25.31	32.85	38.04	44.84	50.09	55.50	68.93
1 hour	38.93	50.54	58.52	68.98	77.06	85.39	106.04

Table 9. IDF (Intensity - Duration - Frequency) curve for M0124

T	Duration of precipitation "t" (mm/h)											
	5 min	10 min	15 min	20 min	25 min	30 min	35 min	40 min	45 min	50 min	55 min	60 min
2 years	197.37	128.75	100.27	83.98	73.19	65.41	59.48	54.78	50.95	47.74	45.02	42.67
5 years	232.20	151.47	117.97	98.80	86.11	76.95	69.98	64.45	59.94	56.17	52.96	50.20
10 years	262.58	171.28	133.41	111.73	97.37	87.02	79.13	72.88	67.78	63.52	59.89	56.76
25 years	308.93	201.51	156.95	131.45	114.56	102.38	93.10	85.74	79.74	74.73	70.46	66.78
50 years	349.34	227.88	177.48	148.64	129.54	115.77	105.28	96.96	90.17	84.50	79.68	75.52
100 years	395.05	257.69	200.70	168.09	146.49	130.92	119.05	109.65	101.97	95.56	90.10	85.40
500 years	525.57	342.83	267.02	223.63	194.89	174.18	158.39	145.87	135.66	127.13	119.88	113.62

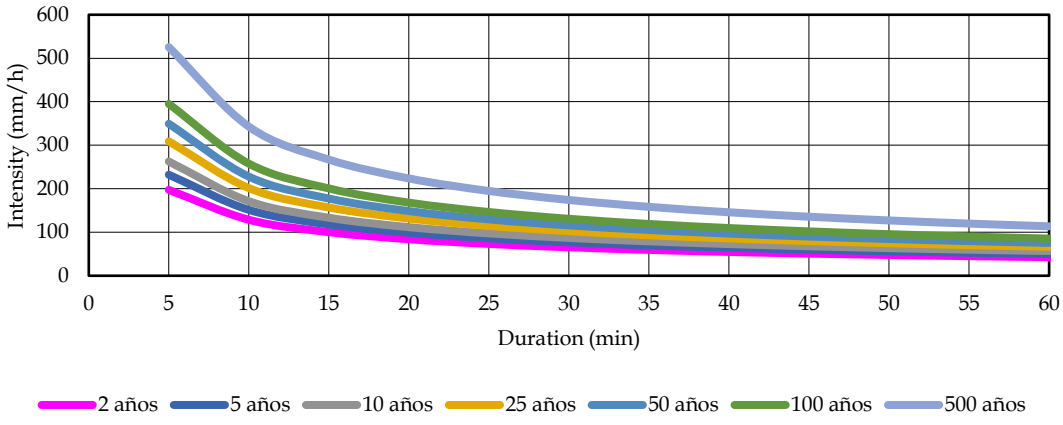

Figure 9. IDF (Intensity - Duration - Frequency) curve for M0124

The results of the statistical analysis in Hydrognomon indicate that the theoretical probability distribution that best fits the annual 24-hour maximum precipitation data from station M0006 is the normal distribution. This finding aligns with the conclusions of Palmer et al. (2024), who asserted that the normal distribution typically provides an adequate representation of maximum annual rainfall data.

However, a contrasting finding emerged from the

statistical analysis conducted in Hydrognomon, which indicated that the Log Pearson III distribution more accurately represented the annual 24-hour maximum precipitation data from station M0124. Furthermore, the Log Pearson III distribution is considered by Rahi et al. (2023) to be a suitable representation of extreme hydrological data, including precipitation and maximum flows. This distribution is adapted to data with a positive bias.

A notable congruence exists between the fundamental objectives of these studies and the research conducted by Shen & Chui (2021) and Thanh-Nhan-Duc & Venkataraman (2024). These studies are oriented towards the inference of potential flood peaks in the event of storms, which have significant socioeconomic ramifications. This justifies the allocation of particular attention to the utilization and occupation of the territory, as well as to the formulation of structural measures for the control of exceptional floods (Zhou et al., 2024). The findings are consistent and offer significant insights into the hydrological and hydraulic design of works in the area (Wang et al., 2024).

4 CONCLUSIONS AND RECOMMENDATIONS

The analysis of the hydroclimatic parameters in the Vinces river basin was conducted using the HYDROGNOMON software, whose methodology was adapted to align with the research objectives. The analysis yielded the IDF curve for varying maximum return periods within the specified basin. The hypothesis was thus confirmed, as the hydroclimatology of the Vinces River basin was thoroughly analyzed.

It is imperative to calibrate and validate the hydrological model to mitigate uncertainty and enhance confidence in the findings. Additionally, it is imperative to ensure the availability of proximate weather stations with historical data to validate the model's outputs.

Hydrometeorological stations play a pivotal role in these initiatives; however, in Ecuador, the number of operational INAMHI stations is inadequate, and there is a need for more systematic maintenance. To address this, it is recommended to utilize global information from reliable organizations.

The utilization of specialized software is also advocated to facilitate the comprehension of the theoretical distribution of probability, a process that integrates numerous statistical evaluations to ascertain the most suitable probability distribution for hydrological and/or meteorological data, contingent upon the prevailing season.

REFERENCES

Allali, H., Elmedahi, Y., Moudjeber, D.-E., Mahmoudi, H., & Goosen, M. F. A. (2022). Utilizing hydrograph transform methods and a hydrologic modeling system in rainfall-runoff simulation of a semi-arid watershed in Algeria in north-west Africa. Desalination and Water Treatment, 255, 220–228. https://doi.org/10.5004/dwt.2022.28344

Arsenault, R., Huard, D., Martel, J.-L., Troin, M., Mai, J., Brissette, F., Jauvin, C., Vu, L., Craig, J. R., Smith, T. J., Logan, T., Tolson, B. A., Han, M., Gravel, F., & Langlois, S. (2023). The PAVICS-Hydro platform: A virtual laboratory for hydroclimatic modelling and forecasting over North America. Environmental Modelling & Software: With Environment Data News, 168(105808), 105808. https://doi.org/10.1016/j.envsoft.2023.105808

Garcia, M., Mohajer Iravanloo, B., & Sivapalan, M. (2024). A diagnostic approach to modeling watersheds with human interference. Journal of Hydrology, 641(131823), 131823. https://doi.org/10.1016/j.jhydrol.2024.131823

Greenwood, W. J., & Eimers, M. C. (2023). Hydroclimatic variability across the international Lake of the Woods watershed: Implications for nutrient export and climate sensitivity. Journal of Great Lakes Research, 49(1), 8–20. https://doi.org/10.1016/j.jglr.2022.12.004

Gunay, C. J. C., Iwama, T., Yokoyama, K., Sakai, H., Kawaue, M., & Takahashi, H. (2024). Impacts of sustainable management on the spatial distributions of erosion susceptibility and probable sediment yield in a mixed-forested watershed. Journal of Environmental Management, 352(119924), 119924. https://doi.org/10.1016/j.jenvman.2023.119924

Hamel, P., Falinski, K., Sharp, R., Auerbach, D. A., Sánchez-Canales, M., & Dennedy-Frank, P. J. (2017). Sediment delivery modeling in practice: Comparing the effects of watershed characteristics and data resolution across hydroclimatic regions. The Science of the Total Environment, 580, 1381–1388. https://doi.org/10.1016/j.scitotenv.2016.12.103

Hao, R., Wang, J., Li, X., Huang, X., Cai, Z. W., & Shi, Z. H. (2023). Cross-timescale interaction of nonstationary hydrological responses in subtropical mountainous watersheds. Journal of Hydrology, 625(130167), 130167. https://doi.org/10.1016/j.jhydrol.2023.130167

Jiang, Z., Tang, M., Yang, X., Wen, H., Yuan, L., Shen, Y., Feng, W., & Zhong, M. (2024). Characterizing multifarious hydroclimatic patterns using geodetic measurements in the Australian mainland. Journal of Hydrology, 642(131792), 131792. https://doi.org/10.1016/j.jhydrol.2024.131792

Lutz, S. R., Mallucci, S., Diamantini, E., Majone, B., Bellin, A., & Merz, R. (2016). Hydroclimatic and water quality trends across three Mediterranean river basins. The Science of the Total Environment, 571, 1392–1406. https://doi.org/10.1016/j.scitotenv.2016.07.102

Mahmood, R., Jia, S., Lv, A., & Babel, M. S. (2024). An integrative analysis of hydroclimatic elements in the three-river source region for historical and future periods: Shift toward an intensified hydrological cycle. International Soil and Water Conservation Research. https://doi.org/10.1016/j.iswcr.2024.01.005

Nasiri-Khiavi, A., Tavoosi, M., Khodamoradi, H., & Kuriqi, A. (2024). Integration of Watershed eco-physical health through Algorithmic game theory and supervised machine learning. Groundwater for Sustainable Development, 26(101216), 101216. https://doi.org/10.1016/j.gsd.2024.101216

Palmer, M. J., Richardson, M., Chételat, J., Spence, C., Connon, R., & Jamieson, H. E. (2024). Watershed hydrology mediates the recovery of an arsenic impacted subarctic landscape. Environmental Pollution (Barking, Essex: 1987), 358(124480), 124480. https://doi.org/10.1016/j.envpol.2024.124480

Prinsloo, F. C., Schmitz, P., & Lombard, A. (2023). System dynamics characterisation and synthesis of floating photovoltaics in terms of energy, environmental and economic parameters with WELF nexus sustainability features. Sustainable Energy Technologies and Assessments, 55(102901), 102901. https://doi.org/10.1016/j.seta.2022.102901

Rahi, A., Rahmati, M., Dari, J., Saltalippi, C., Brogi, C., & Morbidelli, R. (2023). Unraveling hydroclimatic forces controlling the runoff coefficient trends in central Italy's Upper Tiber Basin. Journal of Hydrology. Regional Studies, 50(101579), 101579. https://doi.org/10.1016/j.ejrh.2023.101579

Shahed Behrouz, M., Sample, D. J., & Nayeb Yazdi, M. (2023). Robustness of storm water management model parameter sets for dry and wet hydroclimatic conditions. Journal of Cleaner Production, 411(137328), 137328. https://doi.org/10.1016/j.jclepro.2023.137328

Shen, M., & Chui, T. F. M. (2021). Characterizing the responses of local floods to changing climate in three different hydroclimatic regions across the United States. Advances in Water Resources, 150(103885), 103885. https://doi.org/10.1016/j.advwatres.2021.103885

Staniszewska, K. J., Reyes, A. V., Cooke, C. A., Miller, B. S., & Woywitka, R. J. (2022). Permafrost, geomorphic, and hydroclimatic controls on mercury, methylmercury, and lead concentrations and exports in Old Crow River, arctic western Canada. Chemical Geology, 596(120810), 120810. https://doi.org/10.1016/j.chemgeo.2022.120810

Thanh-Nhan-Duc, T., & Venkataraman, L. (2024). Enhancing human resilience against climate change: Assessment of hydroclimatic extremes and sea level rise impacts on the Eastern Shore of Virginia, United States. The Science of the Total Environment, 947(174289), 174289. https://doi.org/10.1016/j.scitotenv.2024.174289

Tran, T.-N.-D., Tapas, M. R., Do, S. K., Etheridge, R., & Lakshmi, V. (2024). Investigating the impacts of climate change on hydroclimatic extremes in the Tar-Pamlico River basin, North Carolina. Journal of Environmental Management, 363(121375), 121375. https://doi.org/10.1016/j.jenvman.2024.121375

Wang, R., Liu, Y., Zhu, L., Bafitlhile, T. M., Wang, R., & Liu, Y. (2024). Tibetan lake change linked to large-scale atmospheric oscillations via hydroclimatic trajectory. The Science of the Total Environment, 951(175465), 175465. https://doi.org/10.1016/j.scitotenv.2024.175465

Zhang, H., Huang, G. H., Wang, D., & Zhang, X. (2011). Multi-period calibration of a semi-distributed hydrological model based on hydroclimatic clustering. Advances in Water Resources, 34(10), 1292–1303. https://doi.org/10.1016/j.advwatres.2011.06.005

Zhou, Y., Liu, X., Zhao, G., Zuo, C., Alofs, K., & Wang, R. (2024). Pathways linking watershed development and riparian quality to stream water quality and fish communities: Insights from 233 subbasins of the Great Lakes region. Water Research, 261(121964), 121964. https://doi.org/10.1016/j.watres.2024.121964